TOXICOLOGICAL SCIENCES **116(1)**, 44–57 (2010)
doi:10.1093/toxsci/kfq106
Advance Access publication April 7, 2010

Monomethylarsonous Acid Produces Irreversible Events Resulting in Malignant Transformation of a Human Bladder Cell Line Following 12 Weeks of Low-Level Exposure

Shawn M. Wnek,*,[1] Taylor J. Jensen,*,† Paul L. Severson,* Bernard W. Futscher,*,† and A. Jay Gandolfi*

*Department of Pharmacology and Toxicology and †Arizona Cancer Center, University of Arizona, Tucson, Arizona 85721

[1]To whom correspondence should be addressed at College of Pharmacy, 1703 East Mabel Street, PO Box 210207, Tucson, AZ 85721. Fax: (520) 626-2466. E-mail: wnek@pharmacy.arizona.edu.

Received December 29, 2009; accepted March 24, 2010

Arsenic is a known human bladder carcinogen; however, the mechanisms underlying arsenical-induced bladder carcinogenesis are not understood. Previous research has demonstrated that exposure of a nontumorigenic human urothelial cell line, UROtsa, to 50nM monomethylarsonous acid (MMA^{III}) for 52 weeks resulted in malignant transformation. To focus research on the early mechanistic events leading to MMA^{III}-induced malignancy, the goal of this research was to resolve the critical period in which continuous MMA^{III} exposure (50nM) induces the irreversible malignant transformation of UROtsa cells. An increased growth rate of UROtsa cells results after 12 weeks of MMA^{III} exposure. Anchorage-independent growth occurred after 12 weeks with a continued increase in colony formation when 12-week exposed cells were cultured for an additional 12 or 24 weeks without MMA^{III} exposure. UROtsa cells as early as 12 weeks MMA^{III} exposure were tumorigenic in severe combined immunodeficiency mice with tumorigenicity increasing when 12-week exposed cells were cultured for an additional 12 or 24 weeks in the absence of MMA^{III} exposure. To assess potential underlying mechanisms associated with the early changes that occur during MMA^{III}-induced malignancy, DNA methylation was assessed in known target gene promoter regions. Although DNA methylation remains relatively unchanged after 12 weeks of exposure, aberrant DNA methylation begins to emerge after an additional 12 weeks in culture and continues to increase through 24 weeks in culture without MMA^{III} exposure, coincident with the progression of a tumorigenic phenotype. Overall, these data demonstrate that 50nM MMA^{III} is capable of causing irreversible malignant transformation in UROtsa cells after 12 weeks of exposure. Having resolved an earlier timeline in which MMA^{III}-induced malignant transformation occurs in UROtsa cells will allow for mechanistic studies focused on the critical biological changes taking place within these cells prior to 12 weeks of exposure, providing further evidence about potential mechanisms of MMA^{III}-induced carcinogenesis.

Key Words: **arsenic; monomethylarsonous acid; bladder cancer; UROtsa; epigenetic.**

Numerous epidemiological studies have demonstrated that long-term exposure to high levels of arsenic may result in pleiotropic toxicities including cancers of the skin, lung, and urinary bladder as well as numerous noncarcinogenic disease states (Brown and Ross, 2002; Chen *et al.*, 1988, 1995; Lewis *et al.*, 1999; National Research Council, 1999, 2001). However, little is known about the effects of low-level arsenic exposure and the overall contribution to bladder carcinogenesis. To focus research on the mechanistic events leading to monomethylarsonous acid (MMA^{III})–induced malignant transformation, the goal of this research was to resolve an earlier timeline in which low-level (50nM) MMA^{III} exposure induces malignant transformation in an immortalized, nontumorigenic human bladder cell line, UROtsa (Bredfeldt et al., 2006). Defining the critical window in which initial cells demonstrate malignant transformation will not only provide further evidence of the carcinogenic potential of MMA^{III} but will allow for the generation of a specific timeline to mechanistically evaluate the critical biological changes taking place within UROtsa cells leading to malignant transformation and the specific chemical mechanisms MMA^{III} is eliciting to alter normal cell function.

The biotransformation of inorganic arsenic to more toxic, trivalent methylated species is believed to play a key role in arsenical-induced carcinogenesis. Research indicates that the trivalent methylated organoarsenicals, MMA^{III} and dimethylarsinous acid (DMA^{III}), are the most toxic forms, having significantly greater toxicity than inorganic arsenicals and pentavalent organoarsenicals (Petrick *et al.*, 2000, 2001; Styblo *et al.*, 2000). Notably, the trivalent metabolite, MMA^{III}, was demonstrated to be 20 times more toxic than arsenite (As^{III}) in mammalian cell lines (Bredfeldt *et al.*, 2004; Styblo *et al.*, 2002). Vahter (1994) determined that MMA^{III} is a key metabolite in humans based on the ability of humans to produce and excrete a large percentage of MMA^{III} relative to other mammalian species. MMA^{III} is of particular interest because this metabolite may account for the toxicity and carcinogenicity associated with arsenic exposure in humans.

The bladder is a common site of arsenical toxicity resulting from systemic exposure and via bioconcentration of both inorganic arsenic and the multiple biomethylated metabolites in the urine (Tapio and Grosche, 2006). The UROtsa cell line has become an accepted model for studying the effects of arsenical exposure on the transitional epithelium of the human bladder because of its phenotypic and morphological similarity with the primary transitional epithelium (Eblin *et al.*, 2008a; Rossi *et al.*, 2001). UROtsa cells were used as a model to investigate the ability of continuous, low-level MMA^{III} to cause malignant transformation from an initial immortalized state. UROtsa cells were derived from normal urothelium and immortalized using the simian virus 40 large T antigen, resulting in a lack of functional p53 expression (Petzoldt *et al.*, 1995; Rossi *et al.*, 2001). Despite the lack of functional p53 upon immortalization, UROtsa cells did not acquire characteristics typically associated with malignant transformation including anchorage-independent growth and tumor formation when heterotransplanted into immunocompromised mice (Petzoldt *et al.*, 1995; Sens *et al.*, 2004), thus allowing for the evaluation of potential MMA^{III}-induced cellular alterations occurring from an immortalized state to a malignant phenotype.

Numerous mechanisms have been previously identified as contributing to arsenical-associated disease states including the alteration of signaling pathways, increased presence of reactive oxygen species, DNA damage, and the perturbation of the epigenome (Eblin *et al.*, 2008b, 2009; Jensen *et al.*, 2008, 2009a, b; Kligerman *et al.*, 2010; Ludwig *et al.*, 1998; Nesnow *et al.*, 2002; Simeonova *et al.*, 2001; Wnek *et al.*, 2009). In particular, previous studies have shown that epigenetic modifications, including histone tail modifications and DNA methylation are altered in a nonrandom fashion during exposure to either MMA^{III} or As^{III} and that these changes were linked to changes in the transcript levels of associated genes (Benbrahim-Tallaa *et al.*, 2005; Jensen *et al.*, 2008, 2009a, b; Xie *et al.*, 2007; Zhao *et al.*, 1997, 2008).

Low-level arsenic exposure (< 50 ppb) is associated with an increased risk for the development of bladder cancer (Crawford, 2008; National Research Council, 1999, 2001). To associate MMA^{III}-induced malignant transformation of UROtsa cells with alterations demonstrated in bladder cancer, two potential biomarkers of invasive bladder cancer, cyclooxygenase-2 (COX-2) and gene promoter "deleted in bladder cancer 1" (*DBC1*), were examined following low-level MMA^{III} exposure. COX-2 has been demonstrated to be upregulated in high-grade, invasive bladder tumors, and *DBC1* silencing has been associated with multiple forms of carcinogenesis including bladder cancer (Izumi *et al.*, 2005; Nishiyama *et al.*, 1999; Wadhwa *et al.*, 2005).

In 2006, Bredfeldt *et al.* was the first to demonstrate that MMA^{III} causes malignant transformation of UROtsa cells after 52 weeks of exposure to 50nM MMA^{III} (URO-MSC52). These cells were characterized by anchorage-independent growth and the ability to form tumors in severe combined immunodeficiency (SCID) mice after 24 and 52 weeks of exposure, respectively. The 52-week model of MMA^{III}-induced malignant transformation within UROtsa cells was modeled after the model by Sens *et al.* (2004) of malignant transformation of UROtsa cells following long-term exposure (52 weeks) to 1μM As^{III}. Based on the finding of Sens *et al.* (2004), initial studies by Bredfeldt *et al.* (2006) focused on the evaluation of critical changes occurring within UROtsa cells following long-term exposure with a very limited evaluation of potential changes occurring early in the exposure of UROtsa cells to chronic, low-level MMA^{III}. The goal of the research herein was to evaluate the duration of MMA^{III} exposure (50nM) necessary to induce the irreversible malignant transformation of UROtsa cells. Generation of a resolved timeline in which UROtsa cells initially obtain malignant properties will allow for the assessment of key mechanistic events leading to MMA^{III}-induced malignant transformation following low-level exposure. To determine the critical period of malignant transformation in UROtsa cells, cellular growth rate, anchorage-independent growth, and the ability of cells to form tumors in SCID mice following low-level exposure to MMA^{III} were assessed. To uncover the molecular mechanisms that may be associated with the early stages of MMA^{III}-induced malignant transformation and to associate the progression into a malignant state following exposure to MMA^{III}, the DNA methylation patterns of known target promoter regions were assessed and specific biomarkers of invasive bladder cancer were examined. Taken together, these data further refine the window of exposure required for a relevant concentration of MMA^{III} to malignantly transform an immortalized human bladder cell line and establish a more highly resolved timeline to mechanistically examine these cells for specific alterations leading to the irreversible transition of UROtsa cells into a malignant state.

MATERIALS AND METHODS

Reagents. Dulbecco's modified eagle medium (DMEM), fetal bovine serum (FBS), antibiotic-antimycotic, and 1× trypsin-EDTA (0.25%) were acquired from Gibco Invitrogen Corporation (Carlsbad, CA). Noble agar was purchased from Sigma-Aldrich (St Louis, MO). Lipopolysaccharide was purchased from Sigma-Aldrich and was used as a positive control for the induction of cyclooxygenase-2 gene and protein expression. Diiodomethylarsine (MMA^{III} iodide, CH_3AsI_2) was prepared by the Synthetic Chemistry Facility Core (Southwest Environmental Health Sciences Center, Tucson, AZ) using the method of Millar *et al.* (1960). Water used in these studies was distilled and deionized.

Dosing solutions. Preparation of dosing solution and procedures were derived from Bredfeldt *et al.* (2006). Pure MMA^{III} was stored in ampules at 4°C. Fresh stock solutions of 25mM MMA^{III} were made and diluted to a final concentration of 5μM prior to dosing (1:100 dilution) to obtain a final concentration of 0.05μM (50nM) MMA^{III}. The level of MMA^{III} used in this study (50nM) represents a relevant concentration as this specific metabolite has been detected in the urine of humans with MMA^{III} levels at or near 50nM exposed to environmentally relevant concentrations of inorganic arsenic in their drinking water (Aposhian *et al.*, 2000; Mandal *et al.*, 2001). All dosing solutions were sterile filtered with a 0.2μM Acrodisc and stored in sealed, sterile tubes at 4°C that were opened only for dosing in a sterile cell culture hood. As previously reported by Gong *et al.* (2001), MMA^{III} solutions in distilled,

TABLE 1
List of Cell Lines Used in This Study

Cell line (acronym used)	Treatment	Exposure (nM)	Duration (weeks)	MMA^{III} removed[a] (weeks)
UROtsa	None	None	None	NA
URO-MSC4	MMA^{III}	50	4	NA
URO-MSC8	MMA^{III}	50	8	NA
URO-MSC12	MMA^{III}	50	12	NA
URO-MSC16	MMA^{III}	50	16	NA
URO-MSC20	MMA^{III}	50	20	NA
URO-MSC24	MMA^{III}	50	24	NA
URO-MSC36	MMA^{III}	50	36	NA
URO-MSC12+12(–)	MMA^{III}	50	12	12
URO-MSC12+24(–)	MMA^{III}	50	12	24
URO-MSC16+8(–)	MMA^{III}	50	16	8
URO-MSC20+4(–)	MMA^{III}	50	20	4

Note. Cell line (acronym), the treatment metal, concentration (exposure), duration of MMA^{III} exposure, and the time URO-MSC cells were cultured in MMA^{III}-free media following removal of MMA^{III} (weeks) for each cell line is shown. URO-MSC12+12(−) indicates UROtsa cells that were continuously exposed to 50nM MMA^{III} for 12 weeks and then cultured for an additional 12 weeks in the absence of MMA^{III} exposure. URO-MSC12+24(−) indicates UROtsa cells that were continuously exposed to 50nM MMA^{III} for 12 weeks and then cultured for an additional 24 weeks in the absence of MMA^{III} exposure. URO-MSC16+8(−) indicates UROtsa cells that were continuously exposed to 50nM MMA^{III} for 16 weeks and then cultured for an additional 8 weeks in the absence of MMA^{III} exposure. URO-MSC20+4(−) indicates UROtsa cells that were continuously exposed to 50nM MMA^{III} for 20 weeks and then cultured for an additional 4 weeks in the absence of MMA^{III} exposure. NA, not applicable, denoting no removal of continuous MMA^{III} exposure from URO-MSC cells.

[a]Denotes the time in which URO-MSC cells were cultured in MMA^{III}-free media following removal of continuous MMA^{III} exposure.

deionized water were stable for approximately 4 months at 4°C with no degradation observed when monitored using high-performance liquid chromatography–inductively coupled plasma mass spectrometry (HPLC-ICP-MS).

Cell culture. UROtsa cells were a generous gift from Drs Donald and Maryann Sens (University of North Dakota). MMA^{III}-exposed UROtsa cells were created in our laboratory as previously described (Bredfeldt *et al*., 2006). Cell culture conditions were derived from those previously described (Bredfeldt *et al*., 2004; Rossi *et al*., 2001). UROtsa cells were cultured in a growth medium of DMEM containing 5% vol/vol FBS and 1% antibiotic-antimycotic. Culture medium was changed every 2 days. Cultured cells were incubated in an atmosphere that was 5% CO_2:95% air at 37°C. Confluent cells were removed from plates via trypsinization with 1× trypsin-EDTA (0.25%), a serine protease used to digest proteins facilitating cellular adhesion, and subcultured at a ratio of 1:3. All UROtsa and MMA^{III}-exposed UROtsa variant cells used in this study tested negative for the presence of mycoplasma contamination. MMA^{III}-treated cells were continuously cultured in a medium enriched with 50nM MMA^{III} and dosed every other day to ensure continuous presence of MMA^{III}. Duration of MMA^{III} in culture after dosing was determined in previous studies (Wnek *et al*., 2009). Explanation of the MMA^{III}-exposed UROtsa cell lines and acronyms used in this study are noted in Table 1. Parallel cultures of UROtsa cells were maintained in MMA^{III}-free medium and served as passage-matched controls. Cell line DNA fingerprinting was conducted on UROtsa and MMA^{III}-exposed UROtsa variant cell lines to verify their identity. Previous studies have evaluated the ability of UROtsa cells to metabolize As^{III} to MMA^{III}, monomethylarsenic acid (MMA^{V}), and dimethylarsinic acid (DMA^{V}). The most abundant metabolite produced in those studies was MMA^{III}. UROtsa cells treated for 24 h with 50nM MMA^{III} did not metabolize MMA^{III} to more toxic products, as detected by HPLC-ICP-MS (Bredfeldt *et al*., 2004). Results demonstrate that MMA^{III} is the chemical responsible for the observed effects as > 90% of the dose remained in the form of MMA^{III}. Dimethylarsinous acid was not detected in these same UROtsa cells treated with 50nM MMA^{III}.

Cell growth kinetics. Growth curves for UROtsa, URO-MSC4, URO-MSC8, URO-MSC12, URO-MSC24, URO-MSC36, URO-MSC12+12(−), and URO-MSC12+24(−) were obtained via trypan blue exclusion assay (Bredfeldt *et al*., 2006). Cells were plated in six-well plates (Greiner Bio One, Monroe, NC) at a density of 2×10^5 cells per well ($n = 4$). Cells were removed from six-well plates with 1× trypsin-EDTA (0.25%) and counted using the Vi-Cell cell viability analyzer (Beckman Coulter, Fullerton, CA). Average growth curves were generated based on changes in cell number after 24, 48, 72, and 96 h for each of the n values. Cell doubling times were calculated using the formula $N/N_0 = e^{kt}$, where N is the cell number at time t, N_0 is the initial cell number (time 0), and k is a constant. The k value was calculated for each time point between 24 and 96 h and an average value used to calculate the time t when $N/N_0 = 2$ similar to methods described by Butterworth *et al*. (2008).

Cell morphology. Cells were cultured on Delta T dishes (Bioptech, Butler, PA) at 5×10^5 cells per plate and allowed to reach ≥ 90% confluence prior to digital imaging via light microscopy. Photographs were taken to assess changes in morphology of all cell lines. Cells plated on Delta T dishes were mounted on the microscope stage, and images were captured using an Olympus IMT-2 inverted microscope, using a ×20 objective. The camera used was a Hamamatsu ORCA-100 CCD camera (chip resolution 1280 × 1024) in bin2 mode, with the actual image resolution set at 640 × 512 using the SimplePCI version 6.5 (Hamamatsu) instrument control software. Plated cells were prepared for photography by removal of culture media and rinsed twice with PBS. Fresh culture medium (DMEM, no sodium pyruvate) without MMA^{III} was added to cell culture dishes. Images of UROtsa, URO-MSC12, URO-MSC24, URO-MSC36, URO-MSC12+12(−), and URO-MSC12+24(−) were obtained and compared with untreated passage-matched UROtsa controls. Average cell diameter (microns) for UROtsa, URO-MSC4, URO-MSC8, URO-MSC12, URO-MSC24, URO-MSC36, URO-MSC12+12(−), and URO-MSC12+24(−) was determined using an automated trypan blue exclusion assay using the Vi-Cell cell viability analyzer (Beckman Coulter). Cells ($n = 3$) were plated in six-well plates (Greiner Bio One) at 5×10^5 cells per plate. Cells were removed from six-well plates with 200 µl 1× trypsin-EDTA (0.25%) and quenched with 800 µl DMEM containing 5% vol/vol FBS and 1% antibiotic-antimycotic. UROtsa cells and MMA^{III}-exposed variants suspended in medium solution obtained spherical configuration allowing for the assessment of the average cell diameter in microns ($n = 3$, with each n value containing a minimum of 100 mean cell counts) determined using the Vi-Cell cell viability analyzer (Beckman Coulter) (Janakiraman *et al*., 2006).

Colony formation in soft agar. UROtsa, URO-MSC4, URO-MSC8, URO-MSC12, URO-MSC16, URO-MSC20, URO-MSC24, URO-MSC36, URO-MSC12+12(–), URO-MSC12+24(–), URO-MSC16+8(–), and URO-MSC20+4(–) cells were assessed for anchorage-independent growth by colony formation in soft agar similar to methods described by Bredfeldt *et al*. (2006). Cells were removed from culture flask with 1× trypsin-EDTA (0.25%) and suspended in DMEM containing 5% vol/vol FBS and 1% antibiotic-antimycotic supplemented with 0.3% agar. The agar enriched with cells was overlaid onto 0.6% agar medium in a 24-well plate with a density of 1×10^4 cells per well. After 14 days of incubation, colonies were manually counted with an Olympus CK2 microscope (Olympus America, Inc., Melville, NY). Data represent colonies counted from five fields chosen at random within each well ($n = 5$) for a total of 25 fields.

SCID mouse colony. A SCID mouse colony was developed at the University of Arizona using original SCID (C.B-17/IcrACCscid) obtained from Taconic (Germantown, NY). The mice were housed in microisolator cages (Allentown Caging Equipment Company, Allentown, NJ) and maintained under specific pathogen-free conditions. The mice were fed NIH-31–irradiated pellets (Tekland Primier, Madison, WI) and drank autoclaved water. Sentinel mice were screened monthly for mycoplasma, mouse hepatitis virus, pinworms,

and Sendai virus via ELISA. Male mice 6–8 weeks of age were bled (200 μl) by retro-orbital puncture in order to screen for the presence of mouse immunoglobulin (Ig) using ELISA. Only mice with Ig levels $\leq$ 20 μg/ml were used for the xenografts experiments.

Tumorigenicity in SCID mouse xenografts. To assess malignant transformation, UROtsa cells (passage matched), URO-MSC12, URO-MSC12+12(–), and URO-MSC12+24(–) cells (10×10^6) were injected sc into the lower right flank of the mouse in a total volume of 100 μl of sterile saline using a 27-gauge needle (Becton Dickinson, Franklin Lakes, NJ). As tumors developed, tumor size was measured twice weekly for tumor volume estimation (mm^3) in accordance with the formula ($a^2 \times b/2$), where a is the smallest diameter and b is the largest diameter with help of the Experimental Mouse Shared Service (EMSS) at the University of Arizona. All procedures were performed in accordance with approved protocols of the University of Arizona Institutional Animal Care and Use Committee.

Isolation of nucleic acids. UROtsa cells were plated (6×10^5 cells per well) in six-well plates (Greiner Bio One) and grown as previously described (Eblin *et al.*, 2008b) in serum-containing media. Nucleic acids were isolated as previously described (Oshiro *et al.*, 2005). Total RNA was isolated from all cells using the RNeasy Mini Kit (Qiagen, Valencia, CA), and genomic DNA was isolated using the DNeasy Blood and Tissue Kit according to the manufacturer's protocol (Qiagen). All samples were quantified using absorbance at 260 nm on the NanoDrop 1000 Spectrophotometer (NanoDrop, Wilmington, DE).

Real-time reverse transcription–PCR. Gene expression was measured using quantitative real-time reverse transcription (RT)–PCR as previously described (Jensen *et al.*, 2008). Total RNA (250 ng) was reverse transcribed to complementary DNA (cDNA) according to manufacturer's protocol (Applied Biosystems, Foster City, CA). Converted cDNA (10 ng) was added to IQ supermix (Bio-Rad, Hercules, CA), gene-specific primers, and fluorescent probes (Roche) and subjected to real-time PCR analysis using Roche UniversalProbe technology (Roche) using the ABI 7500 Real-Time Detection System (Applied Biosystems). Results were calculated using the delta, delta *Ct* method normalizing to glyceraldehyde 3-phosphate dehydrogenase (GAPDH) expression for each sample. Primers were designed using Primer3 in conjunction with ProbeFinder version 2.40 software (Roche Applied Science). Statistics were calculated using an unpaired *t*-test between each transformed cell line and UROtsa. Primer sequences are available upon request.

COX-2 Western blot analysis. UROtsa, URO-MSC4, URO-MSC8, URO-MSC12, URO-MSC16, URO-MSC12+12(–), and URO-MSC12+24(–) cells were plated in six-well plates (Greiner Bio One) at a density of 1×10^6 cells per well. Cells were removed from six-well plates with 1× trypsin-EDTA (0.25%) quenched with DMEM containing 5% vol/vol FBS and 1% antibiotic-antimycotic, centrifuged, and washed with cold PBS. The cell pellet was resuspended in radioimmunoprecipitation lysis buffer containing 50mM Tris-HCl (pH 8.6), 1% nonyl phenoxylpolyethoxylethanol, 0.25% $C_{24}H_{39}NaO_4$, 150mM NaCl, 1mM PMSF, l g/ml aprotinin, l g/ml leupeptin, 1mM NaF, 1mM Na_3VO_4, 1mM EDTA, and l g/ml protease inhibitor cocktail. The lysates were sonicated and centrifuged at 14,000 rpm for 10 min at 4°C. Supernatant protein concentrations were determined by the Bicinchoninic Acid Kit for protein determination (Sigma-Aldrich). Thirty micrograms of each sample was loaded onto 12% SDS/polyacrylamide gels. Samples were separated via SDS-PAGE with Mini-Protean II (Bio-Rad) and transferred onto polyvinylidene difluoride membranes (Amersham Pharmacia Biotech, Inc./GE Healthcare, Piscataway, NJ) and blocked overnight at 4°C with 5% nonfat dry milk in Tris-buffered saline Tween-20. Blots were incubated overnight at 4°C with primary antibodies for COX-2 (Cayman Chemical, Inc., Ann Arbor, MI) and alpha-Tubulin (Cell Signaling Technology, Danvers, MA) at manufacturer's recommended dilution. The appropriate secondary antibody linked to horseradish peroxidase was used for detection of primary antibody. Chemiluminescent detection was performed with enhanced chemiluminescence Western blotting substrate (Pierce Biotechnology, Inc., Rockford, IL, or GE Healthcare). Images were scanned with a Scanjet 5370C (Hewlett Packard, Palo, Alto, CA) at maximum resolution and prepared in Adobe Photoshop 3.0 (San Jose, CA). Data shown were representative of a total of six experiments ($n = 6$).

DNA methylation analysis by MassARRAY. MassARRAY analysis was performed as previously described (Jensen *et al.*,2009 a, b; Novak *et al.*, 2009). Sodium bisulfite–treated genomic DNA was prepared according to manufacturer's instructions (Zymo Research, Orange, CA). Sodium bisulfite–treated DNA (5 ng) was seeded into a region-specific PCR reaction incorporating a T7 RNA polymerase sequence as described by the manufacturer (Sequenom, San Diego, CA). Resultant PCR product was then subjected to *in vitro* transcription and RNase A cleavage using the MassCLEAVE T-only kit, spotted onto a Spectro CHIP array, and analyzed using the MassARRAY Compact System matrix assisted laser desorption/ionization-time of flight mass spectrometer (Sequenom). Each sodium bisulfate–treated DNA sample was processed in at least two independent experiments. Data were analyzed using EpiTyper software (Sequenom). Primer sequences were designed using EpiDesigner (http://www.epidesigner.com). Primer sequences are available upon request.

Statistics. Graphs were generated in Microsoft Office Excel (Microsoft Corp., Redmond, WA) or in an R programming environment (R Development Core Team, 2007). Cell growth kinetics/cell doubling time analyzed included an $n = 4$ for each experimental value. Statistical significance in average cell diameter was determined from an $n = 3$, with a minimum of 100 mean cell counts assessed per each n value. Soft agar data represent colonies counted from five fields chosen at random within each well ($n = 5$) for a total of 25 fields. Data from tumorigenicity studies represent an average of four experiments. Western blot data for COX-2 represent a total of six experiments. Error bars within each column represent ± SEM unless noted otherwise in figure legends. Statistical analysis utilized and p value cutoff for each experiment is noted in corresponding figure legends.

RESULTS

MMA^{III}-Induced Hyperproliferation of UROtsa Cells

Previous studies have demonstrated malignant transformation of UROtsa cells with both As^{III} (1μM) and MMA^{III} (50nM) after chronic (~52 weeks) exposure (Bredfeldt *et al.*, 2006; Sens *et al.*, 2004). To determine the critical period in the malignant transformation of UROtsa cells following 50nM MMA^{III} exposure, cellular growth rate was assessed. Growth rate was assessed in UROtsa cells exposed to 50nM MMA^{III} for 4, 8, 12, 24, and 36 weeks (Fig. 1a). Untreated UROtsa cells (passage-matched to 52 weeks) had a cell doubling time of approximately 38 h. No significant changes in doubling time were observed after 4 and 8 weeks MMA^{III} exposure; however, after 12 weeks of MMA^{III} exposure (URO-MSC12), there is a ~30% decrease in cell doubling time to 26 h. When the duration of continuous MMA^{III} exposure is carried out to 24 and 36 weeks, cell doubling time remained similar to that of URO-MSC12 cells. Cell doubling time remains decreased upon removal of MMA^{III} as demonstrated in URO-MSC12+12(–) and URO-MSC12+24(–) cells compared with parental UROtsa control (Fig. 1b). The doubling times of URO-MSC12+12(–) and URO-MSC12+24(–) cells slightly increase compared with URO-MSC12 cells; however, the doubling time of these cells do not revert to that of control UROtsa cells upon removal of MMA^{III}.

MMA^{III}-Induced Morphological Changes in UROtsa Cells

The morphology of untreated parental UROtsa cells has been extensively studied by Rossi *et al.* (2001) and is comparable to

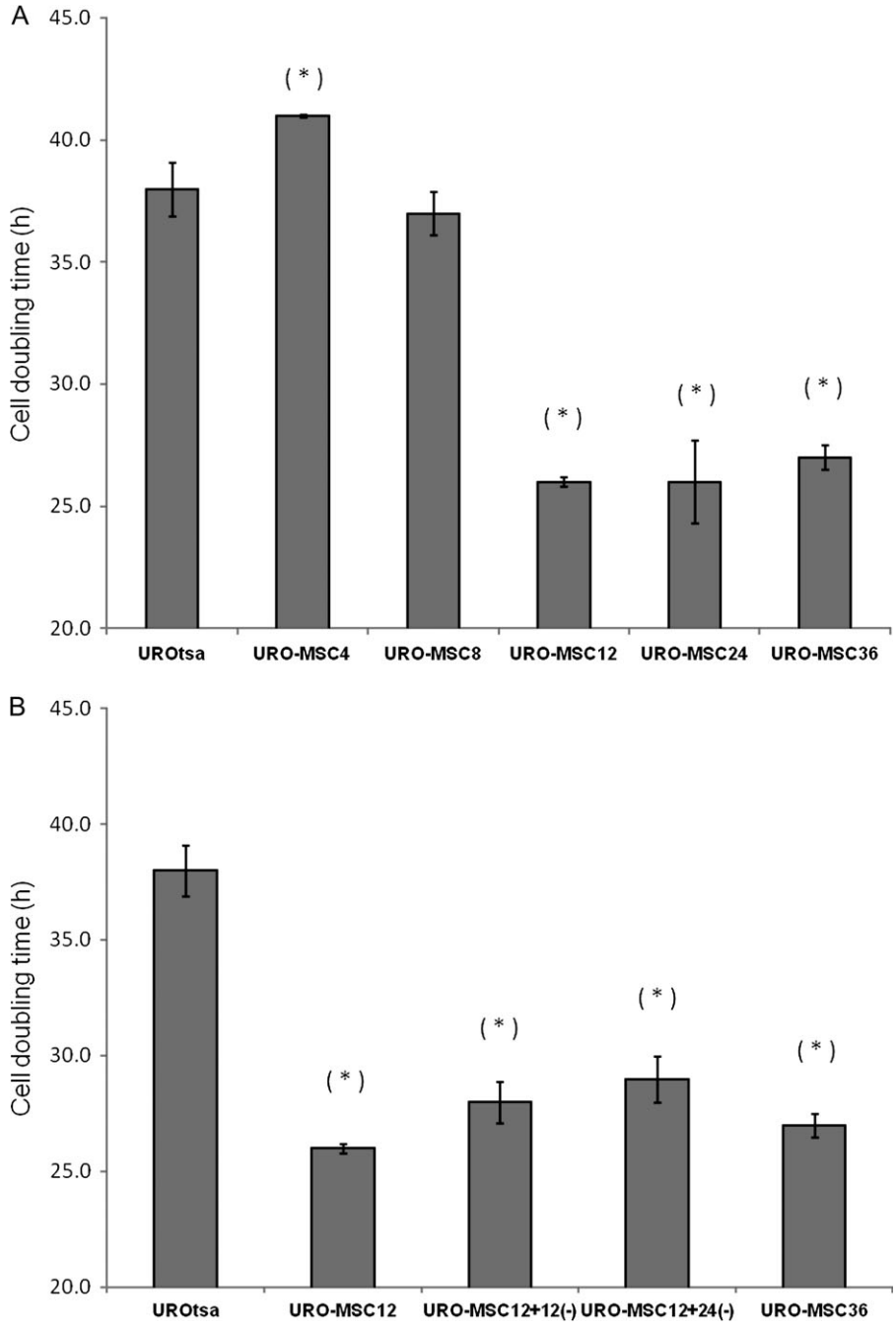

FIG. 1. Cell doubling times following exposure to MMA^{III}. (a) Comparison of cell doubling times of UROtsa control cells and UROtsa cells continuously exposed to 50nM MMA^{III}. A significant decrease in cell doubling time is first demonstrated after UROtsa cells are exposed to 50nM MMA^{III} for 12 weeks (URO-MSC12) and doubling times remain decreased with prolonged continuous exposure to 50nM MMA^{III} through 24 and 36 weeks exposure (URO-MSC24 and URO-MSC36, respectively). (b) Comparison of cell doubling time of UROtsa cells exposed to 50nM MMA^{III} for 12 weeks (URO-MSC12) and 12-week MMA^{III}-exposed UROtsa cells cultured for an additional 12 or 24 weeks without MMA^{III} exposure (URO-MSC12+12(–) and URO-MSC12+24(–), respectively). Cell doubling times remain decreased compared with parental UROtsa in URO-MSC12+12(–) and URO-MSC12+24(–) cells despite the removal of previous MMA^{III} exposure. ''*'' Marks statistically significant difference ($p \leq 0.05$) between MMA^{III}-exposed UROtsa variants (URO-MSC#) and untreated UROtsa control determined using Student's *t*-test.

the control UROtsa cells utilized within this study. UROtsa cells and MMA^{III}-exposed variants were examined via light microscopy to determine whether morphological changes were present in MMA^{III}-exposed UROtsa cells (see Supplementary fig. 1). Within this study, 12-week MMA^{III}-exposed UROtsa cells analyzed via light microscopy demonstrated characteristics similar to those described by Bredfeldt *et al.* (2006) including a less defined cell membrane, the presence of multinucleated

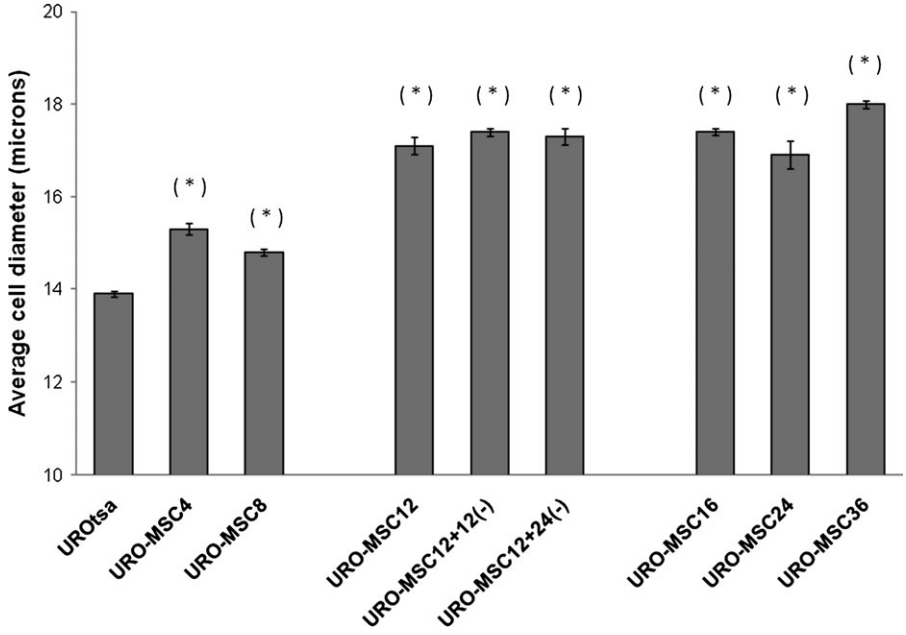

FIG. 2. Cell diameter changes following exposure to MMA^{III}. Average cell diameter (microns) of untreated UROtsa control and UROtsa cells exposed to 50nM MMA^{III} for 4, 8, 12, 24, and 36 weeks (URO-MSC4, URO-MSC8, URO-MSC12, URO-MSC24, URO-MSC36, respectively) and 12-week exposed UROtsa cells with an additional cell culturing without MMA^{III} for 12 and 24 weeks (URO-MSC12+12(–) and URO-MSC12+24(–), respectively). Increase in cell diameter is significantly elevated following 4 weeks exposure to MMA^{III} and remains significantly elevated with prolonged exposure to MMA^{III} through 36 weeks. ''*'' Marks statistically significant difference ($p \leq 0.05$) between MMA^{III}-exposed UROtsa variants (URO-MSC#) and untreated UROtsa control determined using Student's *t*-test.

cells (up to three nuclei per cell), and an overall increase in the nuclear to cytoplasmic ratio. When cell size was examined, a significant increase in the cell diameter of URO-MSC4 cells was demonstrated compared with passage-matched UROtsa. Cell size continues to increase through 12 weeks of exposure (URO-MSC12). Following 12 weeks of MMA^{III} exposure, cell diameter remains stable with continuous exposure to MMA^{III} through 36 weeks (Fig. 2). When MMA^{III} exposure was removed from 12-week MMA^{III}-exposed UROtsa cells and cultured for an additional 12 or 24 weeks without MMA^{III}, cell size remains increased and comparable with URO-MSC12 and URO-MSC36 cells.

MMA^{III}-Induced Anchorage-Independent Growth of UROtsa Cells

Anchorage-independent growth is a phenotype displayed by many tumorigenic cell lines. Measurement of *in vitro* colony-forming ability allows for the assessment of anchorage-independent growth. To determine if the increases in cell proliferation rates and altered morphology were associated with anchorage-independent growth, UROtsa cells exposed to 50nM MMA^{III} for 4, 8, 12, 24, and 36 weeks were tested for the ability to form colonies in soft agar (Fig. 3a). No colony formation was detected in UROtsa cells after 4 and 8 weeks of exposure to 50nM MMA^{III}; however, colony formation was first noted at 12 weeks of MMA^{III} exposure (URO-MSC12). Colony formation continued to increase in a time-dependent manner with prolonged exposure following 16, 20, 24, and 36 weeks exposure to MMA^{III}. Interestingly, when 12-week MMA^{III}-exposed UROtsa cells were removed from MMA^{III} exposure and cultured for an additional 12 or 24 weeks in the absence of MMA^{III} (URO-MSC12+12(–) and URO-MSC12+24(–), respectively) colony formation increased in a time-dependent manner (Fig. 3b, column I). Early anchorage-independent growth was validated when UROtsa cells exposed to 50nM MMA^{III} for 16 and 20 weeks were cultured in the absence of MMA^{III} for an addition 8 and 4 weeks (URO-MSC16+8(–) and URO-MSC20+4(–), respectively) to a total of 24 weeks. Colony growth of URO-MSC16+8(–) cells increased significantly compared with URO-MSC16 cells (Fig. 3b, column II), whereas the colony growth of URO-MSC20+4(–) was similar to that of the URO-MSC20 cells. The number of colonies formed in URO-MSC12+24(–) cells was similar to levels seen in URO-MSC24 cells.

Enhanced Tumorigenicity in UROtsa Cells Following 12-Week, Low-Level Monomethylarsonous Acid Exposure

A common method for determining the degree of malignancy is to examine the tumorigenicity of cells when injected into immunocompromised mice (Saiga *et al.*, 1981). Because significant colony formation was demonstrated in URO-MSC12, URO-MSC12+12(–), and URO-MSC12+24(–) cells compared with untreated UROtsa control, tumorigenicity of these cells was then examined to determine if tumor formation

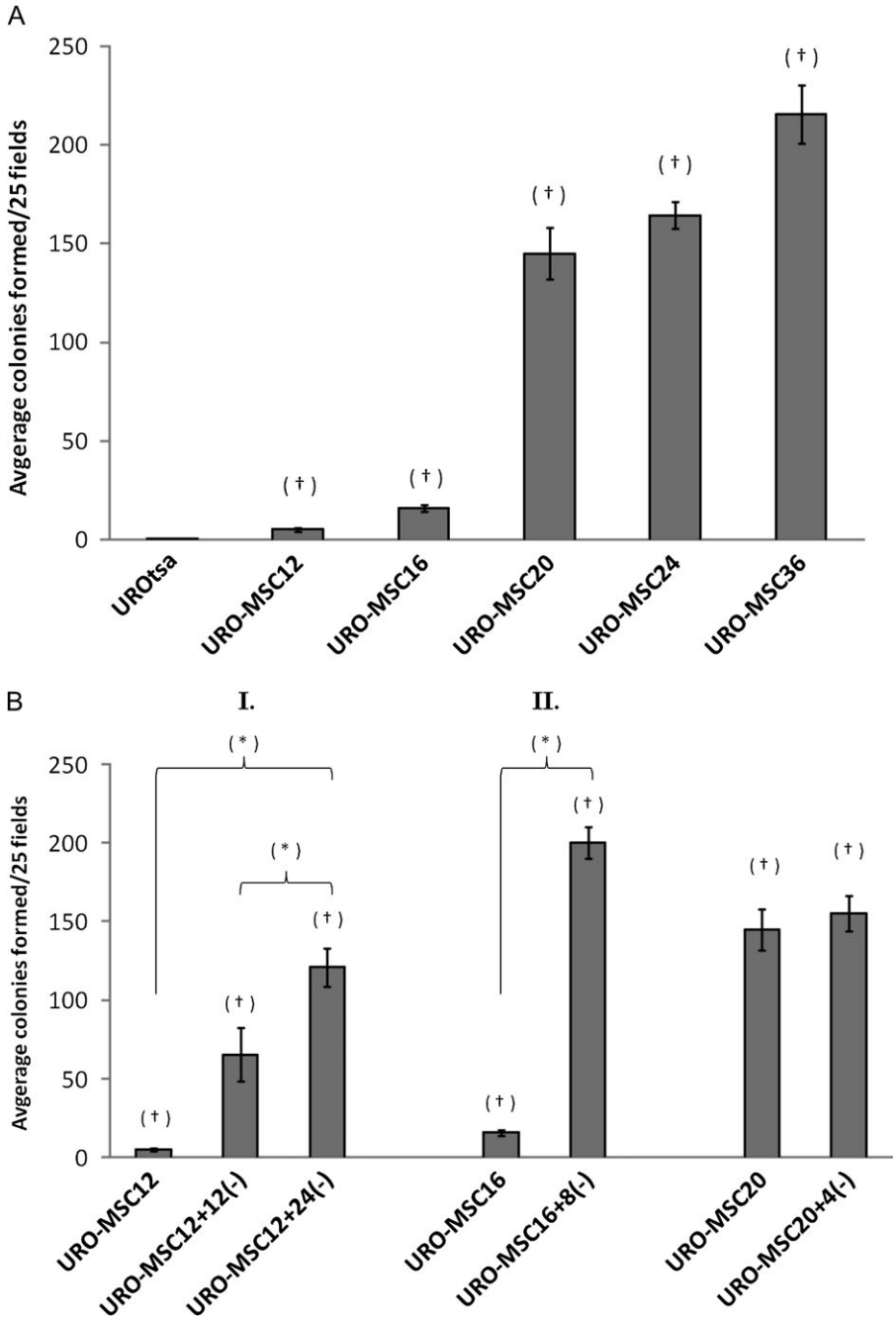

FIG. 3. Anchorage-independent growth following exposure to MMA^{III}. (a) Anchorage-independent growth of UROtsa cells following 4, 8, 12, 16, 20, 24, and 36 weeks exposure to 50nM MMA^{III} (URO-MSC4, URO-MSC8, URO-MSC12, URO-MSC16, URO-MSC20, URO-MSC24 and URO-MSC36, respectively). No colony formation was detected in UROtsa cells after 4- or 8-week MMA^{III} exposure. (b) Comparison of anchorage-independent growth of URO-MSC cells in the presence or following removal of previous exposure to MMA^{III}. Graphs depict colony growth after 14 days incubation in soft agar. Within each well, 5 randomly selected microscope fields were selected and colonies were manually counted from each of the wells ($n = 5$). ''*'' Marks statistically significant difference ($p \leq 0.05$) using Student's *t*-test. ''†'' Marks statistically significant change in the number of colonies formed between MMA^{III}-exposed UROtsa variants (URO-MSC#) and untreated UROtsa control identified with ANOVA followed by Bonferroni's multiple comparison test; $p \leq 0.05$ was considered statistically significant. Error bars within each column represent ± SEM.

occurred following 12 weeks of exposure (URO-MSC12) and whether tumorigenicity increased when these cells were removed from MMA^{III} exposure (URO-MSC12+12(–) and URO-MSC12+24(–), respectively). Passage-matched untreated UROtsa cells were utilized as a negative control because previous work has demonstrated that these cells do not form tumors when injected into SCID mice (Petzoldt *et al.*, 1995; Sens *et al.*, 2004). Tumors were formed by all injected cell lines

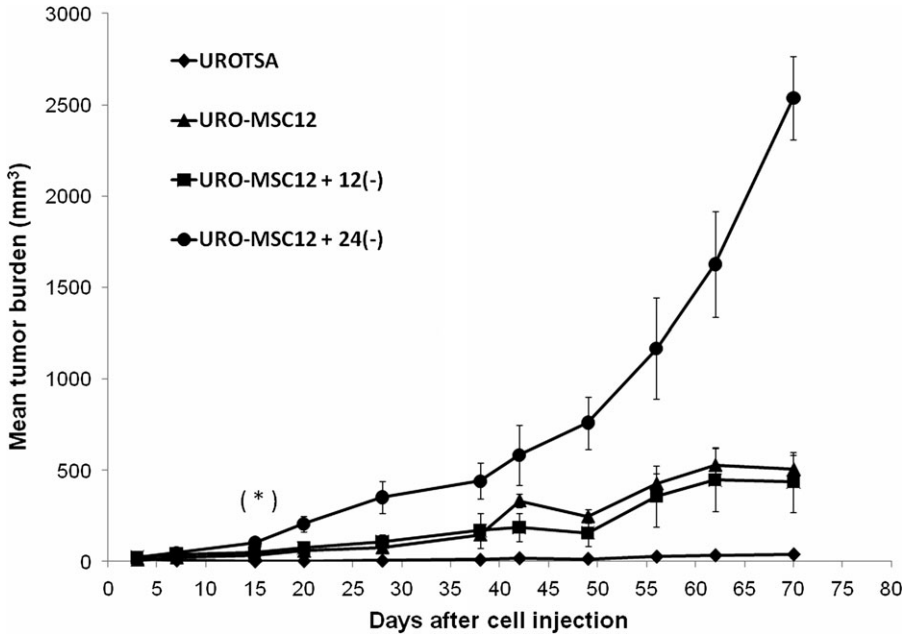

FIG. 4. Tumorigenicity of MMA^{III}-exposed UROtsa variants and untreated UROtsa control in SCID mice. UROtsa, URO-MSC12, and 12-week MMA^{III}-exposed UROtsa cells cultured in the absence of MMA^{III} for 12 or 24 weeks (URO-MSC12+12(–) or URO-MSC12+24(–), respectively) were injected into SCID mice and allowed to grow for 10 weeks to assess tumorigenicity. Tumor volumes were measured twice weekly and data represents tumor volume (mm^3) per time (days postinjection). Mean tumor burden represents the average tumor volume of four independent experiments ($n = 4$). Significant changes in tumor volume were identified with ANOVA followed by Bonferroni's multiple comparisons test. Statistically significant ($p \leq 0.05$) differences in tumor volume of URO-MSC12, URO-MSC12+12(–), and URO-MSC12+24(–) compared with untreated UROtsa control were identified 15 days after injection for each of the MMA^{III}-exposed cell lines. Error bars indicate the SEM at each time point for each cell line. Error bars of untreated UROtsa control are too small to visualize.

with the exception of UROtsa control (Fig. 4). Injection of URO-MSC12 and URO-MSC12+12(–) resulted in significant tumor formation above UROtsa control; furthermore, the greatest tumor formation was demonstrated in URO-MSC12+24(–) cells. Previous studies by Bredfeldt *et al.* (2006) have demonstrated that significant tumors formed following 52 weeks exposure to 50nM MMA^{III}; in the present study, some tumor formation is first noted within URO-MSC12 cells; however, tumorigenic potential increases significantly when URO-MSC12 cells are cultured in the absence of MMA^{III} for 24 weeks.

Epigenetic Changes Associated with MMA^{III}-Induced Progression of Malignant Transformation

The DNA methylation patterns of UROtsa, URO-MSC12, URO-MSC12+12(–), and URO-MSC12+24(–) were assessed as a potential underlying mechanism associated with the malignant transformation of UROtsa cells following 50nM MMA^{III} exposure to a malignant state. The DNA methylation status of five gene promoter regions (*KRT7, FAM83A, GOS2, EREG,* and *THEM4*) previously identified to be progressively methylated during arsenical-mediated malignant transformation of UROtsa cells (Jensen *et al.*, 2009a) were analyzed in UROtsa, URO-MSC12, URO-MSC12+12(–), and URO-MSC12+24(–) cells within the current study. Results from the MassARRAY analysis shows that DNA methylation in each of these promoter regions increases during the progression of UROtsa cells from immortality to malignancy (Fig. 5a). Although DNA methylation changes in these promoters were not detected in URO-MSC12 compared with untreated UROtsa cells, the level of DNA methylation increases as URO-MSC12 cells are cultured for an additional 12 or 24 weeks in the absence of MMA^{III}. Indeed, unsupervised clustering analysis reveals this relationship and suggests that DNA methylation patterns exhibit a relationship between these cells that closely mirrors their tumorigenic potential (Fig. 5b). The progression of DNA methylation levels is associated with characteristics of anchorage-independent growth and tumorigenicity in SCID mice demonstrated within the malignantly transformed URO-MSC12, URO-MSC12+12(–), and URO-MSC12+24(–) cell lines. To determine whether these changes in DNA methylation were linked to changes in the transcript levels of the associated gene, quantitative real-time RT-PCR was performed on parental UROtsa cells and MMA^{III}-exposed UROtsa variants (URO-MSC12, URO-MSC12+12(–), and URO-MSC12+24(–)). The transcript levels of *KRT7, FAM83A, GOS2, EREG,* and *THEM4* each confirmed to be differentially methylated were assessed. Expression levels of those genes that exhibited progressive hypermethylation also exhibited a loss in gene expression (Fig. 5c). Taken together, these data indicate that MMA^{III}-induced aberrant DNA methylation is linked to changes

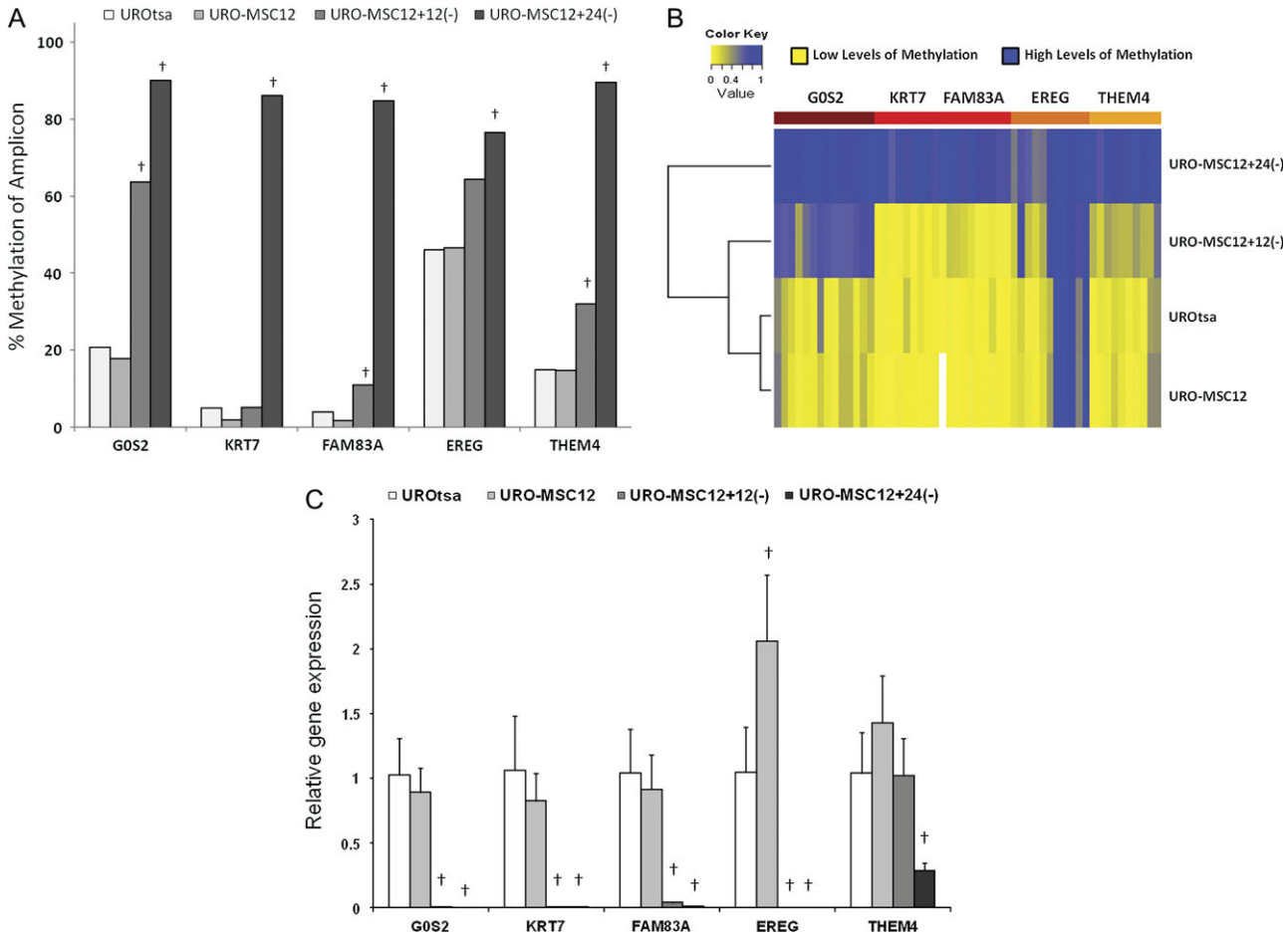

FIG. 5. MMA^{III}-mediated differential DNA methylation in UROtsa cells. (a) Bar chart of MassARRAY data identified MMA^{III}-mediated differential DNA methylation. DNA methylation levels in parental UROtsa cells and each of the MMA^{III}-exposed cell lines (URO-MSC12, URO-MSC12+12(–), URO-MSC12+24(–)) were assessed in five differentially methylated gene promoter regions using Sequenom MassARRAY. The values presented show the average percent CpG methylation of CpG fragments analyzed for each promoter region. ''†'' Marks statistically significant increase in percent methylation of amplicon when compared with control UROtsa ($p \leq 0.05$). (b) Heatmap of MassARRAY data shows MMA^{III}-mediated differential DNA methylation. The heatmap shows the level of cytosine methylation within the individual CpG units on x-axis with yellow representing low levels of methylation and blue representing high levels. Unsupervised hierarchical clustering along the left side shows the progression of DNA methylation is able to discriminate and correctly classify the increasing tumorigenic potential of UROtsa cells to URO-MSC12+24(–) cells. Colors within the top bar represent each of the promoter regions analyzed. (c) Decreased gene expression is linked to MMA^{III}-mediated aberrant DNA hypermethylation of the target gene promoters. Quantitative real-time RT-PCR was performed with $n = 3$ from parental UROtsa and each of the MMA^{III}-exposed variants. ''†'' Marks statistically significant change in transcript level when compared with control UROtsa ($p \leq 0.05$). Values shown are relative to GAPDH normalized to UROtsa.

in gene expression following MMA^{III}-induced malignant transformation, and these changes may play a role in the observed malignant transformation.

Biomarkers of Invasive Bladder Cancer Are Associated with MMA^{III}-Induced Malignant Transformation of UROtsa Cells

Two biomarkers associated with human bladder cancer are the overexpression of COX-2 and the loss of *DBC1* expression. COX-2 is a key enzyme in the synthesis of prostaglandins from arachidonic acid and demonstrated to be involved in various human diseases, including inflammation and cancer (Dannenberg *et al.*, 2001; Subbaramaiah *et al.*, 1997). In particular, overexpression of COX-2 has been implicated to have a role in bladder carcinogenesis (Eschwege *et al.*, 2003; Ristimaki *et al.*, 2001; Shariat *et al.*, 2003; Shirahama, 2000). Although gene expression of URO-MSC cells is similar to that of control after 4 weeks and decreases after 8 weeks of MMA^{III} exposure, following 12 weeks of exposure *COX-2* gene expression is elevated and continues to increase through 16 weeks in the presence of MMA^{III} (Fig. 6a). Interestingly, when 12-week MMA^{III}-exposed UROtsa cells are removed from MMA^{III}, *COX-2* gene expression decreases in a time-dependent manner in URO-MSC12+12(–) and URO-MSC12+24(–) cells, respectively, with expression of URO-MSC12+24(–) cells significantly decreased below control UROtsa. In the presence of MMA^{III}, COX-2 protein levels are elevated above that of control

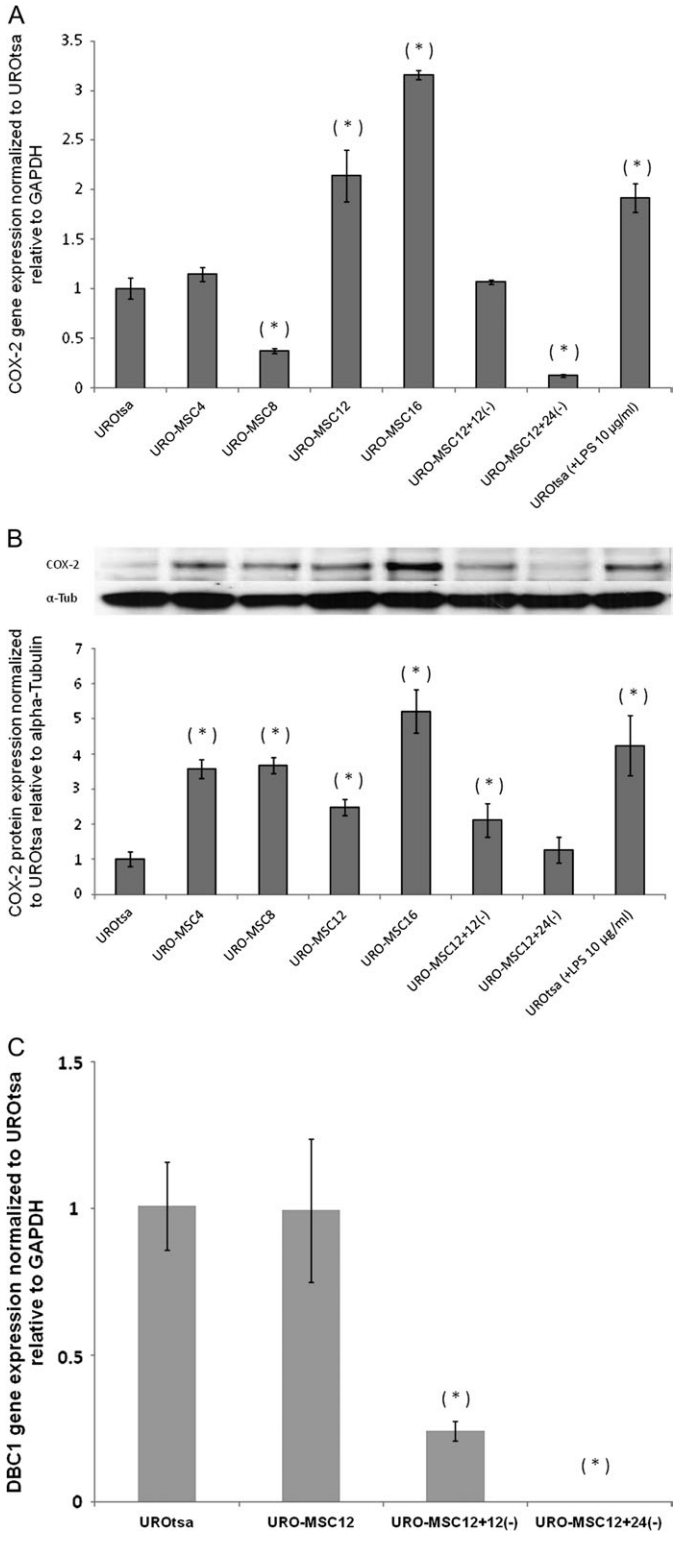

FIG. 6. Assessment of specific biomarkers of invasive bladder cancer in UROtsa cells following 50nM MMA^{III} exposure. (a) Quantitative real-time RT-PCR expression of COX-2 mRNA normalized to UROtsa and relative to GAPDH in parental UROtsa and MMA^{III}-exposed UROtsa variants. ''*'' Marks statistically significant increase/decrease in transcript level when compared with control UROtsa ($p \leq 0.05$); $n = 3$ for all treatment groups. (b) COX-2 protein expression of parental UROtsa cells and MMA^{III}-exposed UROtsa variants. Incubation of UROtsa cells with lipopolysaccharide (10 µg/ml) for 6 h was utilized as a positive control for the induction of COX-2. ''*'' Marks statistically significant increase/decrease in protein levels when compared with control UROtsa ($p \leq 0.05$); $n = 6$ for all treatment groups. (c) Quantitative real-time RT-PCR expression of DBC1 mRNA normalized to UROtsa and relative to GAPDH in parental UROtsa and MMA^{III}-exposed UROtsa variants. ''*'' Marks statistically significant decrease in transcript level when compared with control UROtsa ($p \leq 0.05$); $n = 3$ for all treatment groups.

UROtsa in URO-MSC cells exposed to MMA^{III} from 4 to 16 weeks, and a time-dependent decrease in COX-2 protein levels occurs in URO-MSC12+12(–) and URO-MSC12+24(–) correlating with the decrease in gene transcript levels (Fig. 6b). Elevation of COX-2 at 12 weeks is consistent with the time period in which these cells begin to form colonies in soft agar and show initial tumorigenicity in SCID mice.

DBC1 is mapped to the chromosome region 9q32–33, a tumor suppressor locus for bladder cancer (Habuchi *et al.*, 2001). *DBC1* has been demonstrated to be silenced through genetic and epigenetic mechanisms in multiple cancers including nonsmall cell lung cancer and bladder cancer (Habuchi *et al.*, 1998; Izumi *et al.*, 2005) and in malignantly transformed, human urothelial cells (Jensen *et al.*, 2008). *DBC1* expression does not see a significant change following 12 weeks of exposure to 50nM MMA^{III}; however, when 12-week MMA^{III}-exposed UROtsa cells are carried out for an additional 12 and 24 weeks in the absence of MMA^{III} exposure, *DBC1* gene expression decreases in a time-dependent manner (Fig. 6c) correlating with the significant progression of tumorigenicity demonstrated in URO-MSC12+24(–) cells.

DISCUSSION

Malignant transformation of various human cell lines has been demonstrated following chronic, low-level arsenic exposure (Achanzar *et al.*, 2002; Bredfeldt *et al.*, 2006; Sens *et al.*, 2004; Wen *et al.*, 2007). In 2006, Bredfeldt *et al.* was the first to demonstrate that MMA^{III} causes malignant transformation in UROtsa cells after 52 weeks of exposure. The 52-week MMA^{III}-induced malignantly transformed cell line was modeled from previous research demonstrating malignant transformation of UROtsa cells following chronic exposure to 1µM As^{III} (Sens *et al.*, 2004). Original studies with MMA^{III} were aimed at assessing whether malignant transformation in UROtsa cells was even possible after 52 weeks and limited the evaluation of this novel model to biological changes that were taking place within UROtsa cells after 24 weeks of continuous MMA^{III} exposure (Bredfeldt *et al.*, 2006). Based on emerging evidence of cellular alterations taking place within UROtsa cells prior to 24 weeks of MMA^{III} exposure, the goal of the research herein was to establish a resolved timeline in which

MMA^{III} exposure may induce initial changes early in the chronic exposure of UROtsa cells leading to malignant transformation.

Epidemiological evidence indicates that increased cell division induced by an external agent, such as arsenic exposure, is a common factor in the pathogenesis of human malignancy (Preston-Martin *et al.*, 1990). During low-level arsenic exposure, adaptation to the effects of continuous arsenic exposure can occur resulting in tolerance to apoptosis (Liu and Waalkes, 2008). Tolerance to arsenicals such as MMA^{III} is a common occurrence in arsenical-induced malignantly transformed cells; this phenomenon may allow for damaged cells to survive apoptosis resulting in increased cellular proliferation as demonstrated with the MMA^{III}-exposed UROtsa cells (Chen *et al.*, 2004; Waalkes *et al.*, 2000). The first phenotypic changes demonstrated in the presence of continuous MMA^{III} exposure were a significant increase in cell growth rates after 12 weeks of exposure. Although there is an increase in the cell doubling times of 12-week MMA^{III}-exposed UROtsa cells cultured in the absence of MMA^{III} exposure for 12 or 24 weeks (URO-MSC12+12(–)/URO-MSC12+24(–)) compared with URO-MSC12 cells, the cell doubling times remain significantly decreased when compared with untreated UROtsa control. The stable reduction in cell doubling time despite removal of MMA^{III} implies that 12-week exposed cells demonstrate initial characteristics of irreversible hyperproliferation (cells do not revert to cell growth rates of control UROtsa) and may represent a critical period in the initial acquisition of a malignant phenotype.

UROtsa cells exposed to MMA^{III} for 12 weeks were characterized by a less defined cell membrane and the presence of multinucleated cells similar to results demonstrated by Bredfeldt *et al.* (2006). Large, multinucleated cells containing enlarged nuclei and multiple large nucleoli are consistent with a known bladder carcinoma cell line (Moore *et al.*, 1978) and are considered an indicator of cellular transformation (Walen, 2004). Interestingly, a key morphological feature that was not demonstrated by previous research was a significant increase in cell size following exposure to MMA^{III}. The increase in cell size at these early time points may be associated with MMA^{III}-induced alterations in growth factor signaling resulting in an increase in the number of cells within S-phase/G_2-phase of the cell cycle, thus representing an increase in the amount of cells undergoing cell division (Cleffman *et al.*, 1979; Monroe and Cambier, 1983).

Colony growth in soft agar and tumor growth when injected into SCID mice are two commonly used end points to characterize malignant transformation (Bredfeldt *et al.*, 2006; Mure *et al.*, 2003; Sens *et al.*, 2004). UROtsa cells following 12 weeks of exposure to MMA^{III} result in initial formation of colonies in soft agar, an exposure length previously noted to have resulted in no colony formation (Bredfeldt *et al.*, 2006). The number of colonies formed significantly increases when MMA^{III} exposure is removed from URO-MSC12 cells, and these cells are cultured for an additional 12 or 24 weeks. These results are corroborated through SCID mice data demonstrating initial tumor formation following injection with URO-MSC12 and URO-MSC12+12(–) cells. Similar to the significant increase in colony formation, URO-MSC12+24(–) cells exhibit evidence of increased tumorigenic potential in SCID mice. The increase in colony formation and tumor growth demonstrated with URO-MSC12+12(–) and URO-MSC12+24(–) suggests the progression of a tumorigenic phenotype and the irreversible acquisition of a malignant phenotype after 12 weeks exposure. The selective growth advantage and clonal expansion of cells having acquired malignant characteristics after 12 weeks of exposure may be a possible explanation for the significant increase in malignant phenotypes formed upon removal of MMA^{III}. Kojima *et al.* (2009) demonstrated that arsenic biomethylation-competent UROtsa cells (UROtsa/F35) acquired a malignant phenotype after 18 weeks of exposure to arsenite; in contrast, UROtsa cells (methylation-deficient) did not acquire characteristics of cellular invasiveness or colony formation until 55 weeks of arsenite exposure. These results strengthen the role of arsenic methylation in toxicity and support our findings of direct MMA^{III} exposure to induce malignant transformation early in the chronic exposure of UROtsa cells (methylation deficient) to this critical metabolite.

MMA^{III}-induced malignant transformation of UROtsa cells is associated with the progressive nature of changes in DNA methylation that occur during the transition of cells from an immortal to malignantly transformed state (Benbrahim-Tallaa *et al.*, 2005; Jensen *et al.*, 2008, 2009a, b; Xie *et al.*, 2007; Zhao *et al.*, 1997; Zhou *et al.*, 2008). To uncover the molecular mechanisms that may be associated with MMA^{III}-induced malignant transformation following 12 weeks of exposure, DNA methylation patterns were assessed. The level of DNA methylation progresses as 12-week MMA^{III}-exposed UROtsa cells are cultured for an additional 12 or 24 weeks after removal of MMA^{III}; furthermore, the DNA methylation patterns are inversely related to the transcript levels of target genes. The alterations in DNA methylation levels in URO-MSC12, URO-MSC12+12(–), and URO-MSC12+24(–) cells are associated with the increases in anchorage-independent growth and tumorigenicity in SCID mice and suggest an early event in the malignant transformation of UROtsa cells following low-level MMA^{III} exposure. The exact mechanisms causing an increase in DNA methylation upon removal of MMA^{III} exposure are unknown. However, early MMA^{III} exposure may be acting to initiate epigenetic changes in a select population of UROtsa cells resulting in a malignant phenotype. Upon removal of MMA^{III}, progeny of UROtsa having acquired a malignant phenotype early in the exposure to MMA^{III} could inherit the malignant phenotype in the absence of MMA^{III} exposure resulting in the increase in DNA methylation patterns demonstrated in URO-MSC12+12(–) and URO-MSC12+24(–) cells removed from previous MMA^{III} exposure. These data are consistent with previous studies evaluating the role of altered DNA methylation patterns following exposure to arsenic (Benbrahim-Tallaa *et al.*, 2005;

Jensen *et al*., 2008, 2009a, b; Xie *et al*., 2007; Zhao *et al*., 1997; Zhou *et al*., 2008) and reinforce the role of an epigenetic component in MMA^{III}-induced malignant transformation.

Biomarkers of invasive bladder cancer appear in UROtsa cells following low-level exposure to MMA^{III} and correlate with malignant transformation. Elevated expression of COX-2 is associated with tumors of the urinary bladder (Eltze *et al*., 2005; Fosslien, 2000; Wadhwa *et al*., 2005). Klein *et al*. (2005) demonstrated that COX-2 overexpression plays a critical role in the development of transitional cell hyperplasia and transitional cell carcinoma of the bladder in transgenic mice. COX-2 has been demonstrated to be associated with mitogenic signaling pathways, suggesting a role for COX-2 in stimulating cell growth (Eblin *et al*., 2007). To our knowledge, the levels of COX-2 upon removal of previous chronic arsenic exposure have not been evaluated, and it appears that the presence of MMA^{III} is necessary for the induction of COX-2 as withdrawal of MMA^{III} has been demonstrated to result in a time-dependent decrease in COX-2 gene and protein levels. However, the upregulation of COX-2 at initial stages of continuous MMA^{III} exposure may act as an inflammatory mediator involved in the initial promotion of cell proliferation and cell invasion. The induction of *DBC1* has been noted to be downregulated in multiple cancers, including bladder cancer (Habuchi *et al*., 1998; Izumi *et al*., 2005). Previous studies have demonstrated *DBC1* to be downregulated in UROtsa cells following chronic (52 week) exposure to 50nM MMA^{III} and correlated with the ability of these cells to form tumors when injected into SCID mice (Jensen *et al*., 2008). In URO-MSC12+24(–) cells, *DBC1* expression is completely abolished; interestingly, these cells demonstrated the greatest tumorigenic potential in SCID mice, suggesting a possible role of *DBC1* as a prognostic indicator of bladder cancer.

Within our model, direct exposure of methylation-deficient UROtsa cells to relevant levels of the methylated metabolite, MMA^{III}, results in the transformation to a malignant phenotype. The acquisition of anchorage-independent growth and tumorigenicity in SCID mice provide evidence that 12 weeks of MMA^{III} exposure is capable of causing irreversible malignant transformation in UROtsa cells. In addition, we demonstrate that aberrant changes in DNA methylation in target gene promoter regions are associated with malignant transformation, and the progression of a malignant phenotype. Critical periods in MMA^{III}-induced malignant transformation are associated with biomarkers for invasive bladder cancer including increased COX-2 levels in the presence of continuous MMA^{III} exposure, and a decrease in *DBC1* transcript levels is associated with enhanced tumorigenicity in URO-MSC12+24(–) cells. Taken together, these studies provide a critical timeline to mechanistically examine the chemical effects of MMA^{III} in exposed UROtsa cells resulting in specific biological alterations leading to the irreversible acquisition of a malignant phenotype prior to 12 weeks exposure.

SUPPLEMENTARY DATA

Supplementary data are available online at http://toxsci.oxfordjournals.org/.

FUNDING

The National Institute of Environmental Health Sciences (NIEHS) Superfund Basic Research Program (ES 04940); Southwest Environmental Health Sciences Center (ES 06694); NIEHS Training (ES 07091 to S.M.W.); NIEHS (CA127989 to B.W.F. and ES 06694 to The Genomics Shared Service); Cancer Biology Training (CA09213 to T.J.J.).

ACKNOWLEDGMENTS

The authors would like to thank Drs Donald and Mary Ann Sens and Dr Scott Garret for the UROtsa cells and assistance with culturing conditions. The authors would like to acknowledge the EMSS Core at the Arizona Cancer Center for assistance with the SCID mouse tumorigenicity studies.

REFERENCES

Achanzar, W. E., Brambila, E. M., Diwan, B. A., Webber, M. M., and Waalkes, M. P. (2002). Inorganic arsenite-induced malignant transformation of human prostate epithelial cells. *J. Natl. Cancer Inst.* **94,** 1888–1891.

Aposhian, H. V., Gurzau, E. S., Le, X. C., Gurzau, A., Healy, S. M., Lu, X., Ma, M., Yip, L.i, Zakharyan, R. A., Maiorina, R. M., *et al*. (2000). Occurrence of monomethylarsonous acid in urine of humans exposed to inorganic arsenic. *Chem. Res. Toxicol.* **13,** 693–697.

Benbrahim-Tallaa, L., Waterland, R. A., Styblo, M., Achanzar, W. E., Webber, M. M., and Waalkes, M. P. (2005). Molecular events associated with arsenic-induced malignant transformation of human prostatic epithelial cells: aberrant genomic DNA methylation and K-ras oncogene activation. *Toxicol. Appl. Pharmacol.* **206,** 288–298.

Bredfeldt, T. G., Jagadish, B., Eblin, K. E., Mash, E. A., and Gandolfi, A. J. (2006). Monomethylarsonous acid induced transformation of human bladder cells. *Toxicol. Appl. Pharmacol.* **216,** 69–79.

Bredfeldt, T. G., Kopplin, M. J., and Gandolfi, A. J. (2004). Effects of arsenite on UROtsa cells: low-level arsenite causes accumulation of ubiquitinated proteins that is enhanced by reduction in cellular glutathione levels. *Toxicol. Appl. Pharmacol.* **198,** 412–418.

Brown, K. G., and Ross, G. L. (2002). Arsenic, drinking water, and health: a position paper of the American Council on Science and Health. *Regul. Toxicol. Pharmacol.* **36,** 162–174.

Butterworth, K. T., McCarthy, H. O., Devlin, A., Ming, L., Robson, T., McKeown, S. R., and Worthington, J. (2008). Hypoxia selects for androgen independent LNCaP cells with a more malignant geno- and phenotype. *Int. J. Cancer* **123,** 760–768.

Chen, C. J., Kuo, T. L., and Wu, M. M. (1988). Arsenic and cancers. *Lancet* **1,** 414–415.

Chen, H., Li, S., Liu, J., Diwan, B. A., Barrett, J. C., and Waalkes, M. P. (2004). Chronic inorganic arsenic exposure induces hepatic global and individual gene hypomethylation: implications for arsenic hepatocarcinogenesis. *Carcinogenesis* **25,** 1779–1786.

Chen, S. L., Yeh, S. J., Yang, M. H., and Lin, T. H. (1995). Trace element concentration and arsenic speciation in the well water of a Taiwan area with endemic blackfoot disease. *Biol. Trace Elem. Res.* **48,** 263–274.

Cleffman, G., Reuter, W. O., and Seyfert, H. M. (1979). Increase in macromolecular amounts during the cell cycle of Tetrahymena: a contribution to cell cycle control. *J. Cell Sci.* **37,** 117–124.

Crawford, J. M. (2008). The origins of bladder cancer. *Lab Invest.* **88,** 686–693.

Dannenberg, A. J., Altorki, N. K., Boyle, J. O., Dang, C., Howe, L. R., Weksler, B. B., *et al.* (2001). Cyclo-oxygenase 2: a pharmacological target for the prevention of cancer. *Lancet Oncol.* **2,** 544–551.

Eblin, K. E., Bredfeldt, T. G., Buffington, S., and Gandolfi, A. J. (2007). Mitogenic signal transduction caused by monomethylarsonous acid in human bladder cells: role in arsenic-induced carcinogenesis. *Toxicol. Sci.* **95,** 321–330.

Eblin, K. E., Bredfeldt, T. G., and Gandolfi, A. J. (2008a). Immortalized human urothelial cells as a model of arsenic-induced bladder cancer. *Toxicology* **248,** 67–76.

Eblin, K. E., Hau, A. M., Jensen, T. J., Buffington, S. E., Futscher, B. W., and Gandolfi, A. J. (2008b). The role of reactive oxygen species in arsenite and monomethylarsonous acid-induced signal transduction in human bladder cells: acute studies. *Toxicology* **250,** 47–54.

Eblin, K. E., Jensen, T. J., Wnek, S. M., Buffington, S. E., Futscher, B. W., and Gandolfi, A. J. (2009). Reactive oxygen species regulate properties of transformation in UROtsa cells exposed to monomethylarsonous acid by modulating MAPK signaling. *Toxicology* **255,** 107–114.

Eltze, E., Wülfing, C., Von Struensee, D., Piechota, H., Buerger, H., and Hertle, L. (2005). Cox-2 and Her2/neu co-expression in invasive bladder cancer. *Int. J. Oncol.* **26,** 1525–1531.

Eschwege, P., Ferlicot, S., Droupy, S., Ba, N., Conti, M., Loric, S., Coindard, G., Denis, I., Ferretti, L., Cornelius, A., *et al.* (2003). A histopathologic investigation of PGE(2) pathways as predictors of proliferation and invasion in urothelial carcinomas of the bladder. *Eur. Urol.* **44,** 435–441.

Fosslien, E. (2000). Molecular pathology of cyclooxygenase-2 in neoplasia. *Ann. Clin. Lab. Sci.* **30,** 3–21.

Gong, Z., Lu, X., Cullen, W. R., and Le, C. (2001). Unstable trivalent arsenic metabolites, monomethylarsonous acid and dimethylarsinous acid. *J. Anal. At. Spectrom.* **16,** 1409–1413.

Habuchi, T., Luscombe, M., Elder, P. A., and Knowles, M. A. (1998). Structure and methylation-based silencing of a gene (DBCCR1) with a candidate bladder cancer tumor suppressor region at 9q32-33. *Genomics* **48,** 277–288.

Habuchi, T., Takahashi, T., Kakinuma, H., Wang, L., Tsuchiya, N., Satoh, S., Akao, T., Sato, K., Ogawa, O., Knowles, M. A., *et al.* (2001). Hypermethylation at 9q32-33 tumour suppressor region is age-related in normal urothelium and an early and frequent alteration in bladder cancer. *Oncogene* **20,** 531–537.

Izumi, H., Inoue, J., Hosoda, H., Shibata, T., Sunamori, M., Hirohashi, S., Inazawa, J., and Imoto, I. (2005). Frequent silencing of DBC1 is by genetic or epigenetic mechanisms in non-small cell lung cancers. *Hum. Mol. Genet.* **14,** 997–1007.

Janakiraman, V., Forrest, W. F., and Seshagiri, S. (2006). Estimation of baculovirus titer based on viable cell size. *Nat Protoc.* **1,** 2271–2276.

Jensen, T. J., Novak, P., Eblin, K. E., Gandolfi, A. J., and Futscher, B. W. (2008). Epigenetic remodeling during arsenical-induced malignant transformation. *Carcinogenesis* **29,** 1500–1508.

Jensen, T. J., Novak, P., Wnek, S. M., Gandolfi, A. J., and Futscher, B. W. (2009a). Arsenicals produce stable progressive changes in DNA methylation patterns that are linked to malignant transformation of immortalized urothelial cells. *Toxicol. Appl. Pharmacol.* **241,** 221–229.

Jensen, T. J., Wozniak, R. J., Eblin, K. E., Wnek, S. M., Gandolfi, A. J., and Futscher, B. W. (2009b). Epigenetic mediated transcriptional activation of WNT5A participates in arsenical-associated malignant transformation. *Toxicol. Appl. Pharmacol.* **255,** 107–114.

Klein, R. D., Van Pelt, C. S., Sabichi, A. L., Dela Cerda, J., Fischer, S. M., Fürstenberger, G., and Müller-Decker, K. (2005). Transitional cell hyperplasia and carcinomas in urinary bladders of transgenic mice with keratin 5 promoter-driven cyclooxygenase-2 overexpression. *Cancer Res.* **65,** 1808–1813.

Kligerman, A. D., Malik, S. I., and Campbell, J. A. (2010). Cytogenetic insights into DNA damage and repair of lesions induced by a monomethylated trivalent arsenical. *Mutat. Res.* **695,** 2–8.

Kojima, C., Ramirez, D. C., Tokar, E. J., Himeno, S., Drobna, Z., Styblo, M., Mason, R. P., and Waalkes, M. P. (2009). Requirement of arsenic biomethylation for oxidative DNA damage. *J. Natl. Cancer. Inst.* **101,** 1670–1681.

Lewis, D. R., Southwick, J. W., Ouellet-Hellstrom, R., Rench, J., and Calderon, R. L. (1999). Drinking water arsenic in Utah: a cohort mortality study. *Environ. Health Perspect.* **107,** 359–365.

Liu, J., and Waalkes, M. P. (2008). Liver is a target of arsenic carcinogenesis. *Toxicol. Sci.* **105,** 24–32.

Ludwig, S., Hoffmeyer, A., Goebeler, M., Kilian, K., Hafner, H., Neufeld, B., Han, J., and Rapp, U. R. (1998). The stress inducer arsenite activates mitogen-activated protein kinases extracellular signal-regulated kinases 1 and 2 via a MAPK kinase 6/p38-dependent pathway. *J. Biol. Chem.* **273,** 1917–1922.

Mandal, B. K., Ogra, Y., and Suzuki, K. T. (2001). Identification of dimethylarsonous and monomethylarsonous acids in human urine of the arsenic-affected areas in West Bengal, India. *Chem. Res. Toxicol.* **14,** 371–378.

Millar, I. T., Heany, H., Heinehey, D. M., and Fernelius, W. C. (1960). Methyliiodoarsine. *Inorg. Synth.* **6,** 113–115.

Monroe, J. G., and Cambier, J. C. (1983). Sorting of B lymphoblasts based upon cell diameter provides cell populations enriched in different stages of cell cycle. *J. Immunol. Methods* **63,** 45–56.

Moore, G. E., Morgan, R. T., Quinn, L. A., and Woods, L. K. (1978). A transitional cell carcinoma cell line. *In Vitro* **14,** 301–306.

Mure, K., Uddin, A. N., Lopez, L. C., Styblo, M., and Rossman, T. G. (2003). Arsenite induces delayed mutagenesis and transformation in human osteosarcoma cells at extremely low concentrations. *Environ. Mol. Mutagen.* **41,** 322–331.

Nesnow, S., Roop, B. C., Lambert, G., Kadiiska, M., Mason, R. P., Cullen, W. R., and Mass, M. J. (2002). DNA damage induced by methylated trivalent arsenicals is mediated by reactive oxygen species. *Chem. Res. Toxicol.* **15,** 1627–1634.

Nishiyama, H., Takahashi, T., Kakehi, Y., Habuchi, T., and Knowles, M. A. (1999). Homozygous deletion at the 9q32-33 candidate tumor suppressor locus in primary human bladder cancer. *Genes Chromosomes Cancer* **26,** 171–175.

National Research Council. (1999). *Arsenic in Drinking Water*. National Academy Press, Washington, DC.

National Research Council. (2001). *Arsenic in Drinking Water: 2001 Update*. National Academy Press, Washington, DC.

Novak, P., Jensen, T. J., Garbe, J. C., Sampfer, M. R., and Futscher, B. W. (2009). Stepwise DNA methylation changes are linked to escape from defined proliferation barriers and mammary epithelial cell immortalization. *Cancer Res.* **69,** 5251–5258.

Oshiro, M. M., Kim, C. J., Wozniak, R. J., Junk, D. J., Munoz-Rodrigues, J. L., Burr, J. A., Fitzgerald, M., Pawar, S. C., Cress, A. E., Domann, F. E., *et al.* (2005). Epigenetic silencing of DSC3 is a common event in human breast cancer. *Breast Cancer* **7,** 669–680.

Petrick, J. S., Ayala-Fierro, F., Cullen, W. R., Carter, D. E., and Aposhian, H. V. (2000). Monomethylarsonous acid (MMA(III)) is more toxic than arsenite in Chang human hepatocytes. *Toxicol. Appl. Pharmacol.* **163,** 203–207.

Petrick, J. S., Jagadish, B., Mash, E. A., and Aposhian, H. V. (2001). Monomethylarsonous acid (MMA(III)) and arsenite: LD(50) in hamsters and in vitro inhibition of pyruvate dehydrogenase. *Chem. Res. Toxicol.* **14,** 651–656.

Petzoldt, J. L., Leigh, I. M., Duffy, P. G., Sexton, C., and Masters, J. R. (1995). Immortalisation of human urothelial cells. *Urol. Res.* **23,** 377–380.

Preston-Martin, S., Pike, M. C., Ross, R. K., Jones, P. A., and Henderson, B. E. (1990). Increased cell division as a cause of human cancer. *Cancer Res.* **50,** 7412–7421.

R Development Core Team. (2007). *R: A Language and Environment for Statistical Computing*. *R Foundation for Statistical Computing*. Vienna, Austria.

Ristimaki, A., Nieminen, O., Saukkonen, K., Hotakainen, K., Nording, S., and Haglund, C. (2001). Expression of cyclooxygenase-2 in human transitional cell carcinoma of the urinary bladder. *Am. J. Pathol.* **158,** 849–853.

Rossi, M. R., Masters, J. R., Park, S., Todd, J. H., Garrett, S. H., Sens, M. A., Somji, S., Nath, J., and Sens, D. A. (2001). The immortalized UROtsa cell line as a potential cell culture model of human urothelium. *Environ. Health Perspect.* **109,** 801–808.

Saiga, T., Adachi, T., Okamoto, E., and Midorikawa, O. (1981). An improved method for calculating colony formation in soft agar with special reference to malignancy. *Experientia* **37,** 310–312.

Sens, D. A., Park, S., Gurel, V., Sens, M. A., Garrett, S. H., and Somji, S. (2004). Inorganic cadmium- and arsenite-induced malignant transformation of human bladder urothelial cells. *Toxicol. Sci.* **79,** 56–63.

Shariat, S. F., Kim, J. H., Ayala, G. E., Kho, K., Wheeler, T. M., and Lerner, S. P. (2003). Cyclooxygenase-2 is highly expressed in carcinoma in situ and T1 transitional cell carcinoma of the bladder. *J. Urol.* **169,** 938–942.

Shirahama, T. (2000). Cyclooxygenase-2 expression is up-regulated in transitional cell carcinoma and its preneoplastic lesions in the human urinary bladder. *Clin. Cancer Res.* **6,** 2424–2430.

Simeonova, P. P., Wang, S., Kashon, M. L., Kommineni, C., Crecelius, E., and Luster, M. I. (2001). Quantitative relationship between arsenic exposure and AP-1 activity in mouse urinary bladder epithelium. *Toxicol. Sci.* **60,** 279–284.

Styblo, M., Del Razo, L. M., Vega, L., Germolec, D. R., LeCluyse, E. L., Hamilton, G. A., Reed, W., Wang, C., Cullen, W. R., and Thomas, D. J. (2000). Comparative toxicity of trivalent and pentavalent inorganic and methylated arsenicals in human cells. *Arch. Toxicol.* **74,** 289–299.

Styblo, M., Drobna, Z., Jaspers, I., Lin, S., and Thomas, D. J. (2002). The role of biomethylation in toxicity and carcinogenicity of arsenic: a research update. *Environ. Health Perspect.* **110,** 767–771.

Subbaramaiah, K., Zakim, D., Weksler, B. B., and Dannenberg, A. J. (1997). Inhibition of cyclooxygenase: a novel approach to cancer prevention. *Proc. Soc. Exp. Biol. Med.* **216,** 201–210.

Tapio, S., and Grosche, B. (2006). Arsenic in the etiology of cancer. *Mutat. Res.* **612,** 215–217.

Vahter, M. (1994). Species differences in the metabolism of arsenic compounds. *Appl. Organomet. Chem.* **8,** 175–182.

Waalkes, M. P., Keefer, L. K., and Diwan, B. A. (2000). Induction of proliferative lesions of the uterus, testes, and liver in swiss mice given repeated injections of sodium arsenate: possible estrogenic mode of action. *Toxicol. Appl. Pharmacol.* **166,** 24–35.

Wadhwa, P., Goswami, A. K., Joshi, K., and Sharma, S. K. (2005). Cyclooxygenase-2 expression increases with the stage and grade in transitional cell carcinoma of the urinary bladder. *Int. Urol. Nephrol.* **37,** 47–53.

Walen, K. H. (2004). Spontaneous cell transformation: karyoplast derived from multinucleated cells produce new cell growth in senescent human epithelial cultures. *In Vitro Cell Dev. Biol. Anim.* **40,** 150–158.

Wen, G., Calaf, G. M., Partridge, M. A., Echiburu-Chau, C., Zhao, Y., Huang, S., Chai, Y., Li, B., Hu, B., and Hei, T. K. (2007). Malignant (neoplastic) transformation of human small airway epithelial cells induced by arsenic. *Mol. Med.* **14,** 2–10.

Wnek, S. M., Medeiros, M. K., Eblin, K. E., and Gandolfi, A. J. (2009). Persistence of DNA damage following exposure of human bladder cells to chronic monomethylarsonous acid. *Toxicol. Appl. Pharmacol.* **241,** 202–209.

Xie, Y., Liu, J., Benbrahim-Tallaa, L., Ward, J. M., Logsdon, D., Diwan, B. A., and Waalkes, M. P. (2007). Aberrant DNA methylation and gene expression in livers of newborn mice transplacentally exposed to a hepatocarcinogenic dose of inorganic arsenic. *Toxicology* **236,** 7–15.

Zhao, C. Q., Young, M. R., Diwan, B. A., Coogan, T. P., and Waalkes, M. P. (1997). Association of arsenic-induced malignant transformation with DNA hypomethylation and aberrant gene expression. *Proc. Natl. Acad. Sci. U.S.A.* **94,** 10907–10912.

Zhou, X., Sun, H., Ellen, T. P., Chen, H., and Costa, M. (2008). Arsenite alters global histone H3 methylation. *Carcinogenesis* **29,** 1831–1836.